The Journal of Physiology

Ageing and muscular dystrophy differentially affect murine pharyngeal muscles in a region-dependent manner

Matthew E. Randolph[1], Qingwei Luo[2], Justin Ho[1], Katherine E. Vest[1], Alan J. Sokoloff[2] and Grace K. Pavlath[1]

[1]*Department of Pharmacology, Emory University, Atlanta, GA 30322, USA*
[2]*Department of Physiology, Emory University, Atlanta, GA 30322, USA*

Key points

- Millions of elderly individuals have dysphagia, a debilitating and life-threatening condition in which the ability to swallow is impaired.
- Several muscles surround the three regions of the pharynx, which are essential for proper swallowing, yet the effects of ageing and disease on these muscles are not well understood.
- We demonstrate that the fibre size of murine pharyngeal muscles is differentially affected by ageing and muscular dystrophy depending on their location within the pharynx.
- Using a mouse model of an age-associated dysphagic disease (oculopharyngeal muscular dystrophy), we show that overexpression of wild-type polyadenylate binding nuclear protein 1 in muscle tissue prevents age-related dysphagia and age-related muscle atrophy of laryngopharyngeal muscles.
- These results demonstrate that mice are an excellent model for studying mechanisms of ageing and disease on pharyngeal muscle physiology, and such studies could lead to new therapies for individuals with dysphagia.

Abstract The inability to swallow, or dysphagia, is a debilitating and life-threatening condition that arises with ageing or disease. Dysphagia results from neurological or muscular impairment of one or more pharyngeal muscles, which function together to ensure proper swallowing and prevent the aspiration of food or liquid into the lungs. Little is known about the effects of age or disease on pharyngeal muscles as a group. Here we show ageing affected pharyngeal muscle growth and atrophy in wild-type mice depending on the particular muscle analysed. Furthermore, wild-type mice also developed dysphagia with ageing. Additionally, we studied pharyngeal muscles in a mouse model for oculopharyngeal muscular dystrophy, a dysphagic disease caused by a polyalanine expansion in the RNA binding protein, PABPN1. We examined pharyngeal muscles of mice overexpressing either wild-type A10 or mutant A17 PABPN1. Overexpression of mutant A17 PABPN1 differentially affected growth of the palatopharyngeus muscle dependent on its location within the pharynx. Interestingly, overexpression of wild-type A10 PABPN1 was protective against age-related muscle atrophy in the laryngopharynx and prevented the development of age-related dysphagia. These results demonstrate that pharyngeal muscles are differentially affected by both ageing and muscular dystrophy in a region-dependent manner. These studies lay important groundwork for understanding the molecular and cellular mechanisms that regulate pharyngeal muscle growth and atrophy, which may lead to novel therapies for individuals with dysphagia.

(Received 30 June 2014; accepted after revision 26 September 2014; first published online 17 October 2014)
Corresponding author G. Pavlath: Emory University, Department of Pharmacology, 1510 Clifton Rd, Room 5027, Atlanta, GA 30322, USA. Email: gpavlat@emory.edu

Abbreviations A10-WT, wild-type A10.1 PABPN1 overexpression transgenic mouse; A17-MUT, mutant A17.1 PABPN1 overexpression transgenic mouse; FVB, Friend leukaemia virus B; H&E, haematoxylin and eosin; MHC, myosin heavy chains; OPMD, oculopharyngeal muscular dystrophy; PABPN1, polyadenylate binding nuclear protein 1; type I, slow twitch oxidative myofibre; type II, fast twitch glycolytic myofibre; WT, wild-type.

DOI: 10.1113/jphysiol.2014.280420

Introduction

Swallowing is a highly complex and co-ordinated reflex regulated through the central nervous system to elicit a synchronized contraction of muscle tissues surrounding the oral, pharyngeal and oesophageal cavities (Donner *et al.* 1985; Rubesin *et al.* 1987; Ertekin & Aydogdu, 2003; Miller, 2008). The swallow reflex prevents the aspiration of food and liquid into the trachea/lungs and the subsequent development of life-threatening pneumonia (Martin *et al.* 1994; Prasse & Kikano, 2009). Almost 16 million people in the United States are affected with dysphagia (Robbins *et al.* 2002), a debilitating and potentially deadly condition involving impairment of the swallow reflex (Logemann, 2007). Swallow impairment is associated with several diseases, including stroke (Lindgren & Janzon, 1991; Miller, 2008), Parkinson's disease (Logemann, 2007), myasthenia gravis (Ertekin *et al.* 1998), pharyngeal myositis (Ertekin & Aydogdu, 2003), DiGeorge syndrome (Eicher *et al.* 2000), advanced stage Duchenne muscular dystrophy (Nozaki *et al.* 2007; Aloysius *et al.* 2008) and oculopharyngeal muscular dystrophy (OPMD) (Taylor, 1915; Victor *et al.* 1962). Additionally, dysphagia is also associated with ageing (Kawashima *et al.* 2004; Logemann, 2007; Prasse & Kikano, 2009). Studies from Japan, the Netherlands and the United Kingdom suggest that 11–16% of the elderly have dysphagia (Bloem *et al.* 1990; Kawashima *et al.* 2004; Eslick & Talley, 2008; Holland *et al.* 2011). One study found that almost 45% of dysphagic elderly individuals reported no history of stroke or overt disease (Kawashima *et al.* 2004), suggesting a high incidence of age-related dysphagia.

Pharyngeal muscles are an essential component of the swallow reflex (Ertekin & Aydogdu, 2003; Miller, 2008). Seven major muscles are responsible for pharyngeal contraction when swallowing (Donner *et al.* 1985; Rubesin *et al.* 1987; Ekberg *et al.* 2009). These muscles arise during vertebrate development from the third and fourth pharyngeal arches (Mootoosamy & Dietrich, 2002; Noden & Francis-West, 2006) and are comprised of the stylopharyngeus, palatopharyngeus, salpingopharyngeus and the superior, middle and inferior pharyngeal constrictor muscles (Dutta & Basmajian, 1960; Himmelreich, 1973; Donner *et al.* 1985; Rubesin *et al.* 1987). The inferior pharyngeal constrictor can be subdivided into the cricopharyngeus and the thyropharyngeus muscles (Donner *et al.* 1985; Rubesin *et al.* 1987). Despite the critical nature of these muscles, few studies have analysed the effects of age and disease on pharyngeal muscles as a group.

Only a few individual pharyngeal muscles have been studied in the context of ageing and dysphagia. To our knowledge, only one report has linked abnormalities in the palatopharyngeus muscle with dysphagia (Kirberger *et al.* 2006). In contrast, the effects of ageing or disease on the inferior pharyngeal constrictor muscles, particularly the cricopharyngeus muscle, have been well studied (Leese & Hopwood, 1986; Hyodo *et al.* 1999; Bachmann *et al.* 2001; Périé *et al.* 2006; Davis *et al.* 2007; Mu *et al.* 2012; Gidaro *et al.* 2013).

One dysphagic disease that directly affects the cricopharyngeus is the autosomal dominant disease, OPMD (Victor *et al.* 1962; Brais *et al.* 1998). OPMD is caused by a polyalanine expansion in the N-terminus of polyadenylate-binding nuclear protein 1 (PABPN1) (Brais *et al.* 1998; Robinson *et al.* 2005), which plays key roles in RNA biogenesis (Banerjee *et al.* 2013). Despite the ubiquitous expression of PABPN1, only a subset of muscles is primarily affected in OPMD: pharyngeal muscles, tongue, levator palpebrae, extraocular muscles and proximal limb muscles (Victor *et al.* 1962; Little & Perl, 1982). The main prognostic factor for patients with OPMD is the dysphagia associated with cricopharyngeal muscle pathology and dysfunction (Victor *et al.* 1962; Blakeley *et al.* 1968; Montgomery & Lynch, 1971; Little & Perl, 1982). Little is known concerning the effects of mutant PABPN1 expression in the other pharyngeal muscles and their potential contribution to pathology.

To gain an integrated view of pharyngeal muscle physiology, we characterized multiple pharyngeal muscles in mice, and tested whether these muscles are differentially affected with age or muscle-specific overexpression of mutant A17 PABPN1 using a mouse model of OPMD. Our studies provide insight into the myofibre composition of murine pharyngeal muscles and reveal variable sensitivity of individual pharyngeal muscles to growth and atrophic changes associated with ageing or muscular dystrophy. Furthermore, we show that both ageing and overexpression of mutant A17 PABPN1 alter swallowing behaviour in mice, while overexpression of wild-type (WT) A10 PABPN1 protects swallow function throughout life. These studies provide a critical foundation for advancing our understanding of molecular mechanisms underlying changes in pharyngeal muscles that occur with age and/or a disease state.

Methods

Ethical approval

All experiments were performed in compliance with the United States National Institutes of Health and in accordance with approved guidelines and ethical approval from Emory University's Institutional Animal Care and Use Committee.

Mice

Both male and female mice at various ages, as indicated for individual experiments, were utilized in

this study. C57BL/6 and FVB mice were purchased from Charles River Laboratories (Wilmington, MA, USA). A10.1 and A17.1 PABPN1 transgenic mice (Davies *et al.* 2005), a mouse model for OPMD, were acquired from Dr David Rubensztein. Polymerase chain reaction was utilized to distinguish mice expressing the A10.1 or A17.1 PABPN1 allele from wild-type littermates using the following primer sequences (F: 5′-GAGCGACATCATGGTATTCCC-3′; R: 5′-AGGACT GACACGTGCTACGA-3′) (Davies *et al.* 2005).

Dissection of pharyngeal tissue

Mice were killed using CO_2 asphyxiation immediately before tissue collection. The mandible and lower jaw were removed, exposing the pharyngeal tissues. For histological analyses, the middle cervical region of the trachea and oesophagus were transected and pharyngeal tissue was collected using blunt dissection rostrally toward the hard palate. Histological samples included the nasal, oral and laryngeal pharynxes, soft palate, larynx, cranial trachea and cranial oesophagus.

Histology/immunohistochemistry

All muscle tissues were frozen in Tissue Freezing Medium (Triangle Biomedical Sciences, Durham, NC, USA) and 10 μm cross sections were obtained using a Leica (Buffalo Grove, IL, USA) CM1850 cryostat. Sections were collected every 80 μm representing the entire pharynx. Myofibre cross-sectional areas of haematoxylin and eosin (H&E) stained sections of palatopharyngeus (naso- and oropharyngeal regions), thyropharyngeus and cricopharyngeus (laryngopharyngeal region) were quantified using ImageJ 1.43u. Four, five or six representative 200× sections were analysed for myofibre cross-sectional areas from the nasal, oral and laryngeal pharynx, respectively, of 2-, 12- or 24-month-old male and female mice. The total number of myofibres analysed for each genotype averaged 1900 for the nasal and oral pharyngeal sections, and 700 for the laryngeal pharynx. Quantification of centrally localized myonuclei was also performed on the aforementioned sections of 2-month-old male and female mice using ImageJ 1.43u.

For immunostaining, sections of pharyngeal and gastrocnemius/soleus muscles were blocked for endogenous peroxidases using 0.3% H_2O_2 in 0.1 M potassium phosphate buffer (pH 7.3) (PBS) for 10 min and then successively washed with PBS. TNB blocking buffer (0.1 M Tris–HCl, pH 7.5, 0.15 M NaCl and 0.5% blocking reagent) (PerkinElmer, Waltham, MA, USA) was then applied to the sections for 30 min at room temperature, followed by blocking of endogenous binding sites using the M.O.M. Kit (Vector Laboratories Inc., Burlingame, CA, USA). Subsequently, tissue sections were incubated for 1 h at room temperature with either primary antibodies or appropriate isotype controls. The following antibody supernatants (Developmental Studies Hybridoma Bank, Iowa City, IA, USA) were used: BA-D5 [myosin heavy chain (MHC) I], N2.261 (MHC I/IIa/Neonatal), SC-71 (MHC IIa), BF-B6 (Embryonic/Neonatal), 6H1 (MHC IIx), and BF-F3 (MHC IIb). Successive washes in 0.05% Tween 20 in PBS (PBS-T) were followed by another 30 min of incubation in TNB. Horseradish peroxidase-conjugated antimouse IgG or IgM (Jackson ImmunoResearch, West Grove, PA, USA) at 4 μg ml^{-1} in TNB buffer was applied for 60 min at room temperature. After washes with PBS-T, sections were incubated with DAB Fast 3,3′-diaminobenzidine (Sigma-Aldrich, St. Louis, MO, USA).

H&E images of pharyngeal muscles were obtained using a BX51 microscope with a 0.16 NA 4× UPlanApo objective (Olympus, Tokyo, Japan) and a MicroFire digital microscope camera using Neurolucida software (MBF Bioscience, Williston, VT, USA). All other images were acquired using an Axioplan microscope with a 0.5 NA 20× Plan-Neofluar objective (Carl Zeiss MicroImaging, Inc., Oberkochen, Germany) and charge-coupled device camera (Carl Zeiss MicroImaging, Inc.) with Scion Image 1.63 (Scion Corp., NIH, USA). All images were globally processed for contrast, size and brightness using Photoshop CS4 (Adobe, San Jose, CA, USA).

Biochemical analysis of myosin heavy chain isoforms

Extraocular, gastrocnemius/soleus, heart and pharyngeal muscles (i.e. the entire pharynx with larynx/trachea removed) were dissected from 2- or 6-month-old male or female C57BL/6 mice. Tongues were collected from day-old postnatal C57BL/6 pups. From each sample, 40–50 mg of tissue was homogenized in 200 μl of PBS containing 5% protease inhibitor cocktail (Sigma-Aldrich). Homogenates were centrifuged at 10,000 g (4°C) for 10 min and the pellets re-suspended in PBS with protease inhibitors for isolation of the MHC fraction. Total protein content was determined by bicinchoninic acid assay (Pierce BCA protein assay; Thermo Fisher Scientific Inc., Waltham, MA, USA).

The gel electrophoresis protocol was modified from Talmadge and Roy (1993). Briefly, we used stacking gels of 4% acrylamide (wt/vol; acrylamide:*N*,*N*′-methylene-bis-acrylamide, 37.5:1), 30% glycerol, 70 mM Tris, 4 mM EDTA, 0.05% *N*,*N*,*N*′,*N*′-tetramethylethylenediamine, 0.4% sodium dodecyl sulphate (SDS) and 0.1% ammonium persulphate; and separating gels of 8% acrylamide (wt/vol; acrylamide:*N*,*N*′-methylene-bis-acrylamide, 50:1), 30% glycerol, 0.2 M Tris, 0.1 M glycine, 0.05% *N*,*N*,*N*′,*N*′-tetramethylethylenediamine, 0.4% SDS, and 0.1% ammonium persulphate. Two electrode buffers were utilized: 50 mM Tris, 75 mM glycine and 0.05%

SDS buffer was used for the lower electrode while a 6× concentrate of the aforementioned solution with 0.12% 2-mercaptoethanol was used for the upper electrode. Laemmli sample buffer (Bio-Rad Laboratories, Hercules, CA, USA) at a 1:1 dilution was used to solubilize proteins. Electrophoresis was performed at 140 V for 22 h at 4°C. One set of gels were stained with Imperial Protein Stain (Thermo Fisher Scientific Inc.), destained with water and visualized using an Epson (Long Beach, CA, USA) Perfection V33 imager.

For MHC immunoblotting, proteins were transferred from SDS-PAGE gels on to Immuno-Blot PVDF membranes (Bio-Rad Laboratories). After incubation in 0.5× blocking buffer (USB Corporation, Cleveland, OH, USA), membranes were incubated overnight with A4.84 (MHC 1) (Developmental Studies Hybridoma Bank) in 0.5× blocking buffer with 0.1% Triton X-100 at 4°C. Membranes were then washed, incubated with IRDye 800CW goat antimouse IgM (Rockland, Gilbertsville, PA, USA) and visualized by Odyssey Infrared Imaging System (LI-COR, Lincoln, NE, USA).

Polyadenylate binding nuclear protein 1 immunoblotting

Whole pharynxes from 2-month-old male mice, with larynx/trachea removed, were homogenized in RIPA-2 buffer (50 mM Tris–HCl, pH 8.0, 150 mM NaCl, 1% NP-40, 0.5% deoxycholic acid, 0.1% SDS) containing protease inhibitors (Mini Complete; Roche, Basel, Switzerland). The homogenate was centrifuged at 3000 g for 30 min, and the supernatant utilized for SDS-PAGE and immunoblotting. Tissue lysates containing 100 μg of protein were loaded on to 12% Mini-PROTEAN TGX gels (Bio-Rad Laboratories) and subsequently transferred to 0.45 μm nitrocellulose membranes (Bio-Rad Laboratories). The membranes were blocked for non-specific binding with 5% non-fat dry milk in Tris-buffered saline and then incubated with primary antibodies against PABPN1 (Apponi *et al.* 2010) and heat shock protein 90 (Santa Cruz, CA, USA) overnight at 4°C. Secondary antibody labelling was performed using species appropriate horseradish peroxidase-conjugated IgG (Jackson ImmunoResearch) for 1 h at room temperature. Enhanced chemiluminescence was utilized to detect antibody binding and densitometry analysis performed using ImageJ 1.43u.

Lick assays

Pharyngeal function was assessed indirectly using lick assays as described by Lever *et al.* (2009). Briefly, food and water were removed from female mice for 14–16 h overnight. Afterwards, room temperature water and one pellet of food were reintroduced. Water was delivered via a sipper tube bottle with a ball-bearing spout. Mice were digitally videoed to capture lick episodes when drinking. Video was captured using a Panasonic (Kadoma, Osaka, Japan) HC-V10 Digital Video Camera, recorded as MP4 files at 60 frames per second, and analysed by two blinded independent reviewers using AVIDEMUX 2.5.4 software (Mean, http://avidemux.sourceforge.net). Lick rates were determined by counting five independent, continuous-lick episodes that spanned 60 frames of video per animal. Data were averaged per mouse and reported in licks per second.

Statistical analyses

Data were analysed for statistical significance using GraphPad Prism version 5 for Macintosh (GraphPad Software, San Diego, CA, USA). For all statistical tests, a 0.05 level of confidence was considered statistically significant. To determine the significance of two factors among multiple groups, data were analysed using two-way ANOVA with Bonferroni post-tests. Mood's median test was applied to non-parametric data to determine statistical differences between sample distributions using Microsoft Excel 2008 for Mac Software.

Results

Identification of murine pharyngeal muscles

The swallow reflex occurs in three phases, namely oral, pharyngeal and oesophageal (Donner *et al.* 1985; Rubesin *et al.* 1987). Each phase involves a unique set of muscles. The pharyngeal phase of the swallow reflex relies on co-ordinated neuromuscular contractions within the oral cavity paired with muscles located in the nasal, oral and laryngeal regions of the pharynx (Donner *et al.* 1985; Rubesin *et al.* 1987). To study the muscles of each pharyngeal region in mice (Fig. 1*A*), we first identified the various pharyngeal muscles histologically. Pharyngeal tissues extending from the rostral soft palate caudally to the mid-cervical trachea/oesophagus were collected for transverse tissue sectioning and histologic examination via H&E staining.

The nasopharynx was defined as beginning at the closure of the pharyngeal epithelial mucosa where both the superior pharyngeal constrictor muscles dorsolaterally (Fig. 1*B*, yellow diamond) and the palatopharyngeal fold comprised of the palatopharyngeus and salpingopharyngeus ventrolaterally form the pharyngeal cavity (Fig. 1*B*, yellow asterisks) (Nakano & Muto, 1985; Rubesin *et al.* 1987). The velopharyngeal opening marked the end of the nasopharynx and beginning of the oropharynx. The oropharynx extended caudally to the pharyngeal aponeurosis of the palatopharyngeal muscle (Rubesin *et al.* 1987). Muscles identified in the oropharynx

included the middle pharyngeal constrictor (Fig. 1*B*, green triangle) and palatopharyngeus (Fig. 1*B*, green asterisks). The laryngopharynx began at the pharyngeal aponeurosis and extended caudally to the first tracheal ring. Muscles identified in the laryngopharynx were the inferior constrictor muscles, thyropharyngeus (Fig. 1*B*, blue circle) and cricopharyngeus (Fig. 1*B*, blue square). These studies demonstrate that pharyngeal muscles are easily identified in mice using histologic sections, allowing for subsequent comparative analyses among the muscles required for the pharyngeal phase of swallowing.

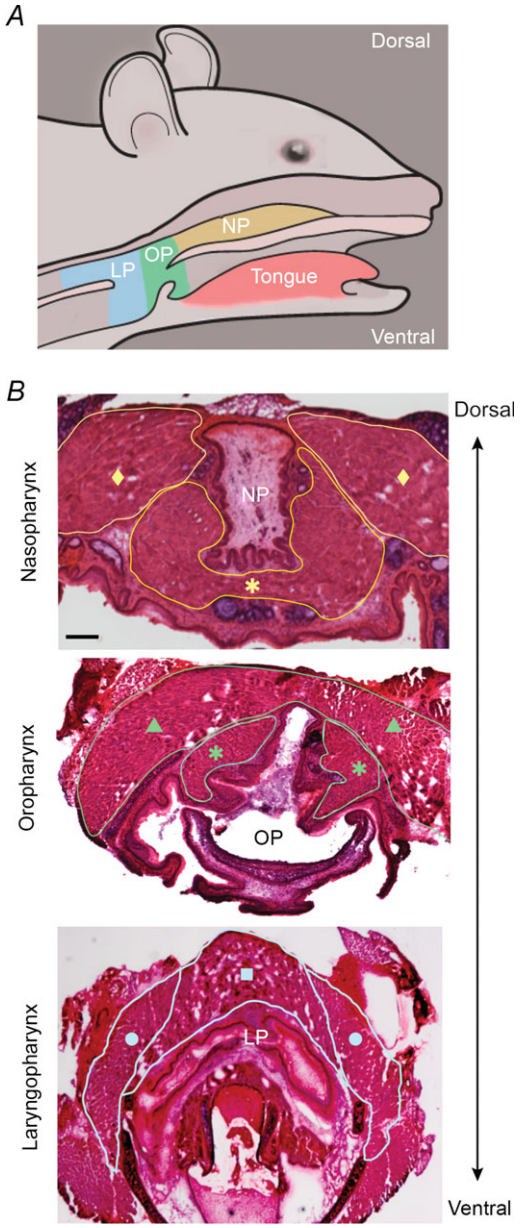

Figure 1. Pharyngeal muscles of mice
A, murine pharyngeal regions depicting the NP in yellow, OP in green, and LP in blue. *B*, representative histologic sections of murine pharyngeal tissue stained with haematoxylin and eosin. Pharyngeal muscles are outlined for identification. Representative images of the NP containing the superior pharyngeal constrictor (♦) and palatopharyngeus (✱); the OP containing the middle pharyngeal constrictor (▲) and palatopharyngeus (✱); and the LP containing the thyropharyngeus (•) and cricopharyngeus (■) are shown. Bar: 250 μm. LP, laryngopharynx; NP, nasopharynx; OP, oropharynx.

Variability in myofibre types between pharyngeal muscles

To examine differences among muscles throughout the pharynx, we began by analysing myofibre types as the myofibre composition of a muscle affects its function. Slow twitch oxidative myofibres (type I) are typically observed in muscles utilized for endurance, whereas the fast twitch glycolytic myofibres (type II) are over-represented in muscles used for rapid contractions (Reiser *et al.* 1985*a*, 1985*b*). Each myofibre type is composed of distinct isoforms of contractile proteins, including MHC. Initially, to determine the myofibre types present in murine pharyngeal muscles as a whole, we isolated MHC proteins and performed separation SDS-PAGE and Coomassie to discriminate myosin isoforms. Mouse pharyngeal muscles predominantly contained type IIb and IIx, and neonatal MHC, with trace amounts of type IIa MHC (Fig. 2*A*). Type I MHC was not detected by either Coomassie stain or immunoblot (Fig. 2*A*). Additionally, neonatal MHC was present in pharyngeal muscles of both young and mature mice (Fig. 2*A*).

To analyse the myofibre composition of individual muscles of the pharynx, we used immunohistochemistry to visualize myofibre types *in vivo*. Type IIb MHC was predominantly expressed in the palatopharyngeus as well as in the superior, middle and inferior pharyngeal constrictor muscles, with lesser amounts of type IIa and IIx. Type I MHC was not observed in any pharyngeal muscle. Immunostaining of representative muscles is shown in Fig. 2*B*. The expression of neonatal MHC was strictly confined to muscles of the inferior constrictor adjacent to the mucosal epithelium of the laryngopharynx (Fig. 2*C*). Thus, murine pharyngeal muscles are mainly composed of fast glycolytic myofibres with neonatal MHC expression confined to the laryngopharynx.

Regional effects of ageing on pharyngeal myofibre size

To study the effects of ageing on the muscles of each pharyngeal region, we performed a histologic study utilizing wild-type FVB mice at 2, 12 and 24 months of age. Myofibre size was determined by analysing cross-sectional areas from the palatopharyngeus (naso- and oropharyngeal regions), thyropharyngeus and cricopharyngeus (laryngopharyngeal region) as these muscles were transected transversely *versus* longitudinally

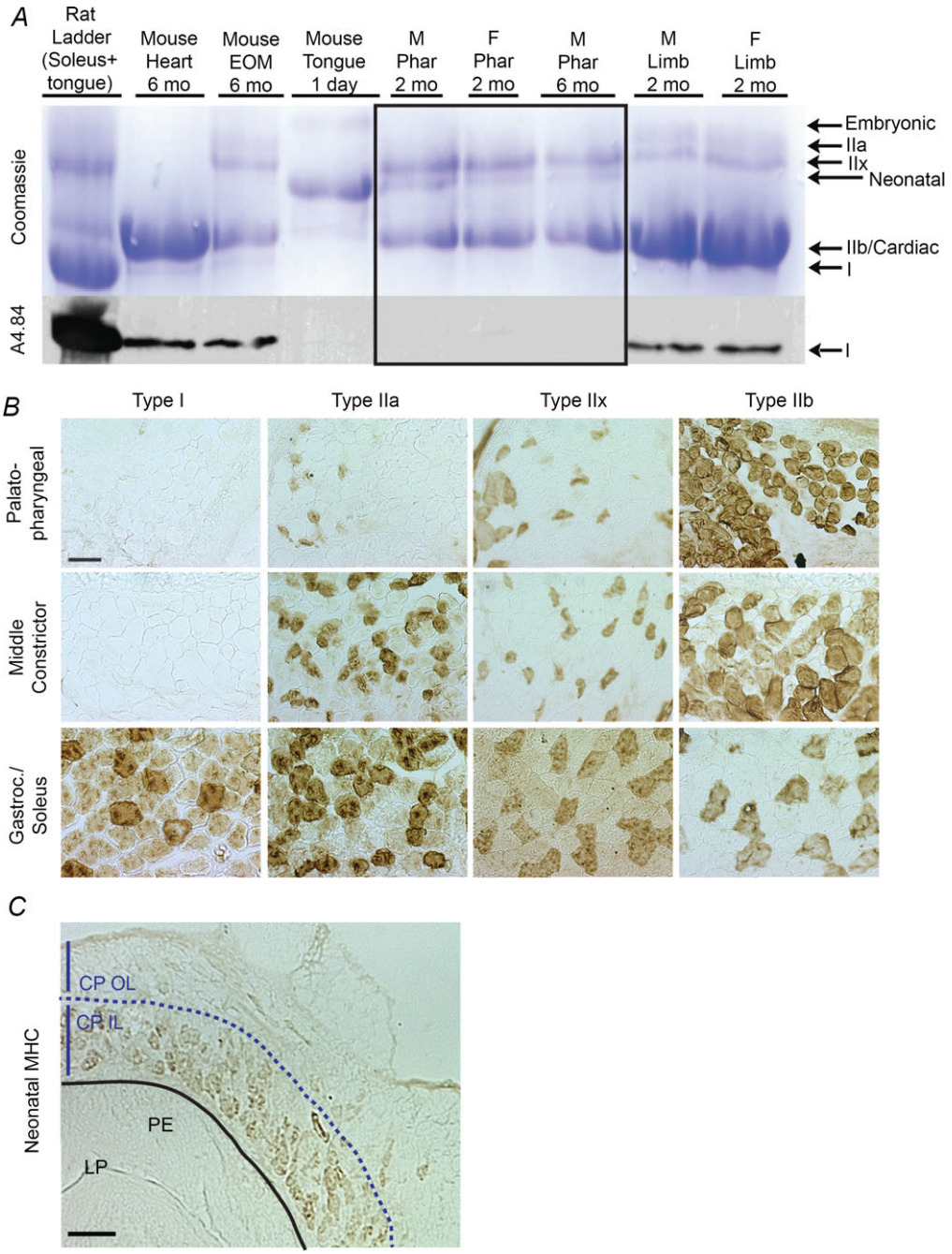

Figure 2. Pharyngeal muscles are composed of fast glycolytic myofibres but lack slow oxidative myofibres

A, MHCs were isolated from the indicated muscles, separated by gel electrophoresis and visualized with coomassie blue (top panel). The main MHCs present in pharyngeal muscles (delineated within the black box) were types IIb and IIx, and neonatal based on comigration with MHC standards from other muscles. No type I MHC was observed in pharyngeal samples, which was confirmed by immunoblot analysis using the type I MHC-specific antibody, A4.84 (bottom panel). $n = 4$ mice pooled per sample. *B*, pharyngeal muscle sections were immunostained with antibodies against type I, IIa, IIx and IIb MHC. Representative sections from the palatopharyngeus and middle pharyngeal constrictor muscle are shown. Gastroc and soleus muscles were used as positive controls. Bar: 50 μm. $n = 3$ mice, 2–3 months of age. *C*, representative image of neonatal MHC immunostaining of the CP muscle in the LP marked with a dashed line to delineate the CP OL and CP IL of the muscle. Bar: 100 μm. $n = 3$ male mice, 2–3 months of age. CP IL, inner layers of the cricopharyngeal muscle; CP OL, outer layers of the cricopharyngeal muscle; EOM, extraocular muscle; F, female; Gastroc, gastrocnemius; LP, laryngopharynx; M, male; MHC, myosin heavy chain; mo, months; PE, pharyngeal epithelium; Phar, pharyngeal muscles.

in sections. From 2 to 12 months of age, significant increases in myofibre size were observed in both the naso- and oropharynx, while myofibre size decreased in the laryngopharynx (Fig. 3*A*). However, by 24 months of age, myofibre size significantly decreased in all three pharyngeal regions (Fig. 3*B*). These results provide evidence that muscles in every pharyngeal region undergo age-related atrophy while muscles of the laryngopharynx undergo atrophy at an earlier age than those in the naso- and oropharynxes.

Overexpression of wild-type A10 and mutant A17 polyadenylate binding nuclear protein 1 has differential effects on pharyngeal muscle growth

We used an OPMD mouse model to test if regional differences in pharyngeal muscle growth or atrophy also occur with muscular dystrophy. This OPMD model overexpresses a 17-alanine-expanded mutant PABPN1 (A17-MUT) specifically in skeletal muscle (Davies *et al.* 2005). Mice overexpressing wild-type PABPN1 (A10-WT), which contains 10 alanines in the N-terminus of the protein, were simultaneously created to control for any effects of overexpressing PABPN1 (Davies *et al.* 2005). The A17-MUT mice develop symptoms of muscle weakness and atrophy with minimal signs of degeneration in limb muscles as early as 6 months of age compared to both wild-type and A10-WT control mice (Davies *et al.* 2005; Trollet *et al.* 2010). As pharyngeal muscles of these mice have never been studied, we first confirmed PABPN1 overexpression in the pharyngeal muscles of both A10-WT and A17-MUT mice relative to wild-type littermates using immunoblots (Fig. 4*A*). A17-MUT mice demonstrated a two-fold increase in PABPN1 overexpression when compared to A10-WT mice (data not shown). The apparent absence of PABPN1 protein in the wild-type pharyngeal muscle is consistent with the findings reported by Apponi *et al.* (2013) that pharyngeal muscles express very low levels of PABPN1 protein compared to limb muscles and other tissues.

Initially, we compared myofibre cross-sectional area of wild-type and A10-WT mice for each region of the pharynx to investigate whether overexpression of wild-type A10 PABPN1 alters pharyngeal muscle growth (Fig. 4*B*). Again, regional differences in pharyngeal myofibre size were observed. At 2 months of age, myofibre size was significantly increased in each pharyngeal region in A10-WT mice (Fig. 4*B*). However, only laryngopharyngeal muscles consistently exhibited increased myofibre size throughout the time course of the experiment (Fig. 4*B*), indicating that overexpression of wild-type A10 PABPN1 both enhances muscle growth and provides resistance to age-related atrophy in laryngopharyngeal muscles.

When analysing the pharyngeal muscle sections from the A10-WT mice, we observed an unusual preponderance of myonuclei with a more central localization within the myofibres, as opposed to the typical subsarcolemmal position. The presence of such centrally

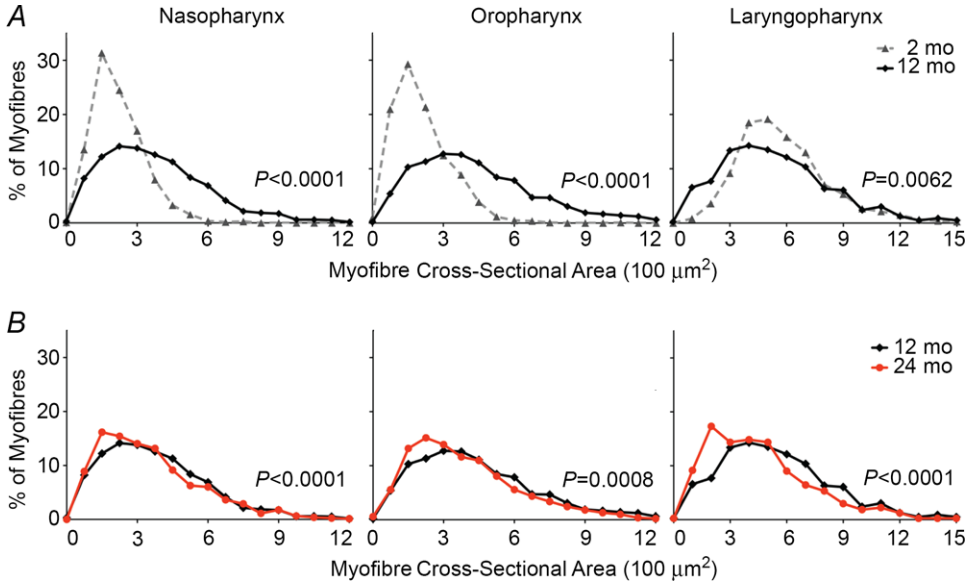

Figure 3. Regional differences in myofibre size occur with ageing in pharyngeal muscles
Histogram plots are shown for myofibre cross-sectional areas (CSA) from the naso-, oro- and laryngopharyngeal regions of wild-type FVB mice at 2, 12 or 24 months of age. *A*, myofibre CSA significantly increased from 2 to 12 months of age in the naso- and oropharynx but decreased in the laryngopharynx. $n = 752–1943$ myofibres, three to four mice per time point. *B*, myofibre CSA decreased from 12 to 24 months of age in all pharyngeal regions. Data from 12 months of age are shown again for comparison. $n = 792–1943$ myofibres, four mice per time point. mo, months.

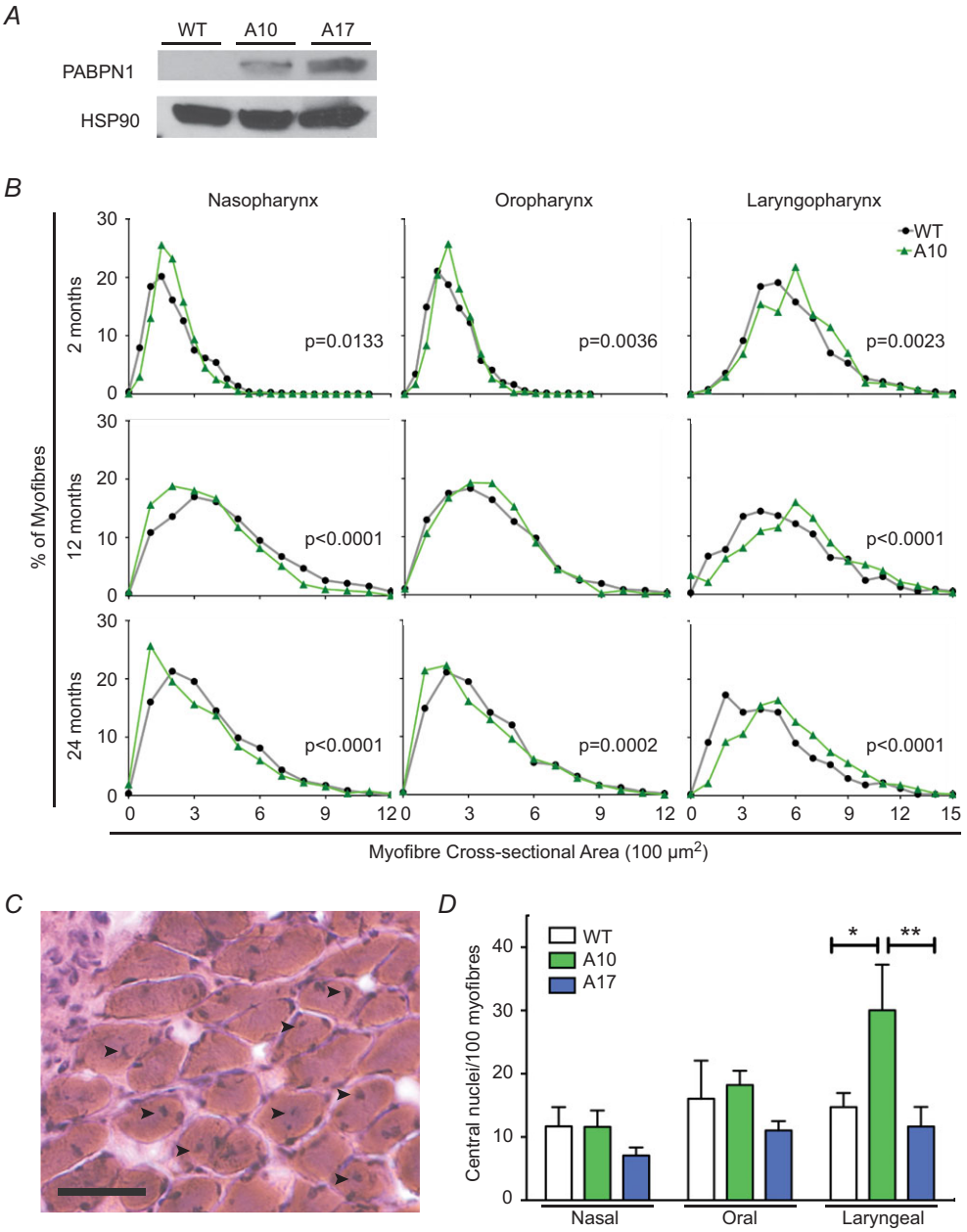

Figure 4. Overexpression of WT A10 PABPN1 enhances muscle growth in only one region of the pharynx
A, representative immunoblot of PABPN1 from pharyngeal muscle lysates of 2-month-old A10-WT, A17-MUT and WT littermates. Lanes were loaded with 100 μg total protein. Heat shock protein 90 was used as a loading control. Data are representative of three independent experiments. *B*, histogram plots are shown for myofibre CSA from the naso-, oro- and laryngopharyngeal regions of WT and A10-WT mice at 2, 12 or 24 months of age. Data from WT mice in Fig. 3 are shown again for comparison. At 2 months of age, overexpression of WT A10 PABPN1 significantly increased myofibre CSA in all three pharyngeal regions. At both 12 and 24 months of age, WT A10 PABPN1 overexpression only increased myofibre size in the laryngopharynx. *P* values are indicated in plots with significant differences in myofibre CSA. $n = 609–1943$ myofibres; three to five mice per genotype and time point. *C*, representative haematoxylin and eosin-stained section of the inferior constrictor muscle located in the laryngopharyx of a WT 2-month-old mouse. Centrally located myonuclei (black arrowheads) are present in multiple myofibres. Bar: 50 μm. *D*, quantification of centrally located myonuclei within the nasal, oral and laryngeal pharynxes of 2-month-old WT, A10-WT and A17-MUT mice. Centrally located myonuclei within A10-WT myofibres were significantly increased compared to WT ($^*P < 0.05$) or A17-MUT ($^{**}P < 0.01$) mice, but only in the laryngopharynx. Data are means ± SEM from 752 to 1214 myofibres from three mice per genotype. A10-WT, wild-type A10.1 PABPN1 overexpression transgenic mouse; A17-MUT, mutant A17.1 PABPN1 overexpression transgenic mouse; CSA, cross-sectional areas; LP, laryngeal pharynx; NP, nasal pharynx; OP, oral pharynx; PABN1, polyadenylate binding nuclear protein 1; WT, wild-type.

located nuclei within myofibres is consistent with myogenesis, the fusion of muscle stem cells with myofibres, resulting in the addition of new myonuclei to myofibres, which contributes to muscle growth (Schmalbruch, 1976). Therefore, we analysed H&E-stained pharyngeal sections of wild-type and A10-WT 2-month-old mice for centrally located myonuclei (Fig. 4*C*). In the naso- and oropharynx, no significant difference in frequency of central nuclei was observed (Fig. 4*D*). However, wild-type A10 PABPN1 overexpression in the laryngopharynx resulted in a significant increase in the incidence of centrally localized nuclei, which was not observed in A17-MUT sections (Fig. 4*D*). These findings suggest that increased levels of wild-type A10 PABPN1 enhance myogenesis in laryngopharyngeal muscles, consistent with the enhanced myofibre size observed in these muscles of A10-WT mice.

Subsequently, we analysed selected pharyngeal muscles (Fig. 3) of A17-MUT mice and compared them to A10-WT mice to control for the variable of PABPN1 overexpression. No signs of myofibre degeneration, immune infiltration or increased interstitial fibrosis were observed in H&E sections (data not shown); however, when myofibre size was quantified for sections from A17-MUT and A10-WT mice at 2, 12 and 24 months of age, overexpression of mutant A17 PABPN1 differentially affected muscle growth and atrophy of specific muscles in each pharyngeal region (Fig. 5). In 2-month-old A17-MUT mice, myofibre size was significantly smaller in the laryngopharynx while minimal changes occurred in the naso- and oropharynx. In 12-month-old A17-MUT mice, major decreases in myofibre size occurred in the oro- and laryngopharynx relative to myofibres from A10-WT mice. Furthermore, when we compared the region of the palatopharyngeus located in the oropharynx at 2 and 12 months, we observed a pronounced impairment of muscle growth demonstrated by failure of A17-MUT myofibres to shift towards a larger size as observed with A10-WT mice between these time points (Fig. 5). This growth impairment between 2 and 12 months was not observed in the nasopharyngeal region of the palatopharyngeus (Fig. 5). By 24 months, no major size differences were observed between A10-WT and A17-MUT myofibres (Fig. 5). Muscles of the oropharynx were more susceptible to the effects of mutant A17 PABPN1 than those in the nasopharynx. Within the muscles of the laryngopharynx, the observed decrease in size with mutant A17 PABPN1 overexpression may be related to pathology caused by the mutant protein. Alternatively, overexpression of the mutant A17 protein may fail to protect against age-related atrophy, as does overexpression of the wild-type A10 protein in laryngopharyngeal muscles. Taken together, these data indicate that variable effects of both age and disease occur in the different regions of the pharynx.

Differential effects of age and overexpression of either wild-type A10 or mutant A17 polyadenylate binding nuclear protein 1 on swallowing

Considering the presence of pharyngeal muscle atrophy with ageing in wild-type mice (Fig. 3), we next hypothesized that swallowing may be impacted by ageing. Currently, no assays exist for directly measuring the pharyngeal phase of swallowing in mice. Therefore, as an indirect test of pharyngeal function, we utilized an assay that analyses the oral phase of swallowing (Lever *et al.* 2009, 2010). In this assay, food and water were withdrawn from mice for 14–16 h. Upon reintroduction of food and water, mice were digitally recorded to visualize individual lick episodes (Fig. 6*A*, Supp. Video 1). Lick rates, defined as the number of licks/second, were quantified for wild-type FVB mice at 6, 18 and 24 months of age (Fig. 6*B*). At 24 months of age, a 9.5% decrease in lick rate occurred in wild-type mice (Fig. 6*B*). We then tested whether age also affects swallowing in A10-WT or A17-MUT mice. Surprisingly, A10-WT mice demonstrated no significant change in lick rates either at 18 or 24 months of age (Fig. 6*C* and *D*). However, at 18 and 24 months of age, A17-MUT mice exhibited decreases in lick rates of 5.9% and 7.2%, respectively, when compared to the A17-MUT 6-month baseline (Fig. 6*D*).

We then tested whether wild-type A10 PABPN1 overexpression provides a protective effect for lick function as was observed in laryngopharyngeal muscle growth (Fig. 4). Therefore, we compared lick rates of A10-WT mice to wild-type mice to determine if increased levels of wild-type A10 PABPN1 significantly altered the ability to swallow. No difference was observed between wild-type and A10-WT lick rates at 6 months of age (Fig. 6*C*). However, A10-WT lick rates were increased, relative to wild-type mice, at both 18 and 24 months of age by 6.2% and 7.3%, respectively.

Finally, we compared the lick rates of A17-MUT mice to the A10-WT overexpression control mice at each time point to determine if mutant A17 PABPN1 expression alters swallow function. No difference in lick rate was observed at 6 months of age (Fig. 6*D*). However, A17-MUT lick rates were impaired relative to A10-WT mice at both 18 and 24 months of age by 8.8% and 6.5%, respectively (Fig. 6*D*). No significant differences in lick rates were observed in A17-MUT mice at any age when compared to wild-type mice (data not shown). The decrease in lick rates observed in A17-MUT mice relative to A10-WT mice could be due to a failure of mutant A17 PABPN1 to rescue age-related dysphagia. Together these data demonstrate that mice develop impaired swallow function both with age and mutant A17 PABPN1 overexpression, while overexpression of wild-type A10 PABPN1 provides a protective effect against age-related dysphagia in mice.

Discussion

Dysphagia is a debilitating condition that affects millions of individuals (Robbins *et al.* 2002), yet little is known about basic pharyngeal muscle biology. Here we utilized a mouse model system to investigate pharyngeal muscles. With age, both pharyngeal muscle atrophy and oral dysphagia developed in wild-type mice. Interestingly, overexpression of wild-type A10 PABPN1 provided protection against the development of age-related dysphagia. Furthermore, we observed differential susceptibility of various pharyngeal muscles to overexpression of either wild-type or mutant A17 PABPN1 in age-related muscle growth and atrophy.

Murine pharyngeal myofibres are composed of type II and neonatal myosin heavy chain

In all murine pharyngeal muscles examined, the predominant myofibre types were fast twitch type II myofibres with no evidence of slow twitch type I myofibres. In contrast, human cricopharyngeal muscle contains a layer of type I myofibres closest to the mucosal epithelium and an outer layer of type II myofibres (Mu & Sanders, 2002; Mu *et al.* 2007). The type I myofibres provide the tonic force for maintaining closure of the upper oesophageal sphincter (Davis *et al.* 2007). Interestingly in murine cricopharyngeal muscle, we observed an inner layer of myofibres expressing neonatal MHC, instead of type I MHC. Other adult craniofacial muscles in mice also express neonatal MHC, such as extraocular muscles (Wieczorek *et al.* 1985), inner ear muscles (Scapolo *et al.* 1991), sternocleidomastoid muscles (McLoon, 1998) and masseter muscles (Butler-Browne *et al.* 1988; Bredman *et al.* 1992). Myofibres expressing neonatal MHC have decreased shortening velocities and strength (Johnson *et al.* 1994), hence they are more similar to slow twitch myofibres than to fast twitch. Thus, the neonatal MHC myofibre layer in murine cricopharyngeal muscle is

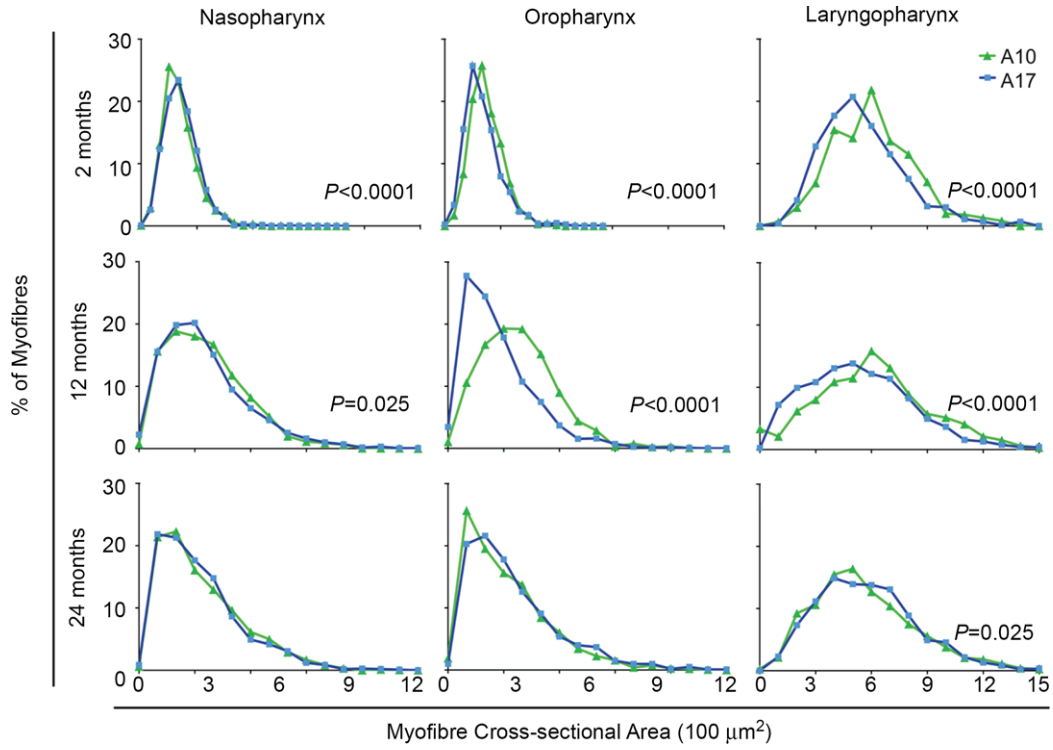

Figure 5. Overexpression of 17-alanine-expanded PABPN1 is deleterious to myofibre size only in specific regions of the pharynx
Histogram plots are shown for myofibre CSA from the naso-, oro- and laryngopharyngeal regions of A10-WT and A17-MUT mice at 2, 12 or 24 months of age. Data from A10-WT mice in Fig. 4 are shown again for comparison. At 2 months of age, myofibre CSA majorly decreased in the laryngopharynx of A17-MUT mice while CSA minimally changed in the naso- and oropharynx. At 12 months of age, major decreases in A17-MUT myofibre CSA occurred in the oro- and laryngopharynx. A pronounced lack of growth occurred in the A17-MUT oropharynx from 2 to 12 months. At 24 months of age, no major differences in myofibre CSA were observed in any pharyngeal region. *P* values are indicated in plots with significant differences in myofibre CSA. $n = 609–2591$ myofibres; three to five mice per genotype and time point. A10-WT, wild-type A10.1 PABPN1 overexpression transgenic mouse; A17-MUT, mutant A17.1 PABPN1 overexpression transgenic mouse; CSA, cross-sectional areas; PABN1, polyadenylate binding nuclear protein 1.

probably functionally analogous to the slow twitch inner myofibre layer of humans.

Postnatal growth and age-related atrophy of murine pharyngeal muscles

In wild-type mice, postnatal muscle growth occurred in muscles of the naso- and oropharynxes followed by late-life muscle atrophy, consistent with age-related muscle growth and atrophy of limb muscles in humans (Aherne *et al.* 1971; Lexell *et al.* 1988; Wada *et al.* 2003). However, muscles of the laryngopharynx reached maximum size in this study by 2 months of age and exhibited muscle atrophy by 12 months of age. These findings point to unique regulatory mechanisms underlying growth of murine laryngopharyngeal muscles in their role as pharyngeal constrictors. To date, postnatal muscle growth in the human laryngopharynx has not been assessed; therefore, whether early onset of laryngopharyngeal muscle atrophy also occurs in humans is unknown. Further studies examining the cellular and molecular mechanisms regulating the differential growth of pharyngeal muscles could provide valuable insights into region-specific differences underlying age-related muscle atrophy of the pharynx.

Wild-type A10 polyadenylate binding nuclear protein 1 overexpression enhances myofibre growth in the laryngopharynx

Davies *et al.* (2008) previously demonstrated that wild-type A10 PABPN1 overexpression in limb muscles protected against OPMD-related apoptosis and strength loss in A17-MUT mice. We observed that overexpression of wild-type A10 PABPN1 alone provided a protective effect on myofibre growth of pharyngeal muscles in a region-dependent manner. Wild-type A10 PABPN1 overexpression enhanced myofibre size in all pharyngeal muscles at 2 months of age, but surprisingly, protected against age-related muscle atrophy only in laryngopharyngeal muscles. These data show that wild-type A10 PABPN1 overexpression differentially affects mechanisms underlying myofibre growth of pharyngeal muscles *in vivo*. Interestingly, recent studies of the vastus lateralis muscle indicate decreased levels of PABPN1 mRNA in the context of both muscle ageing and

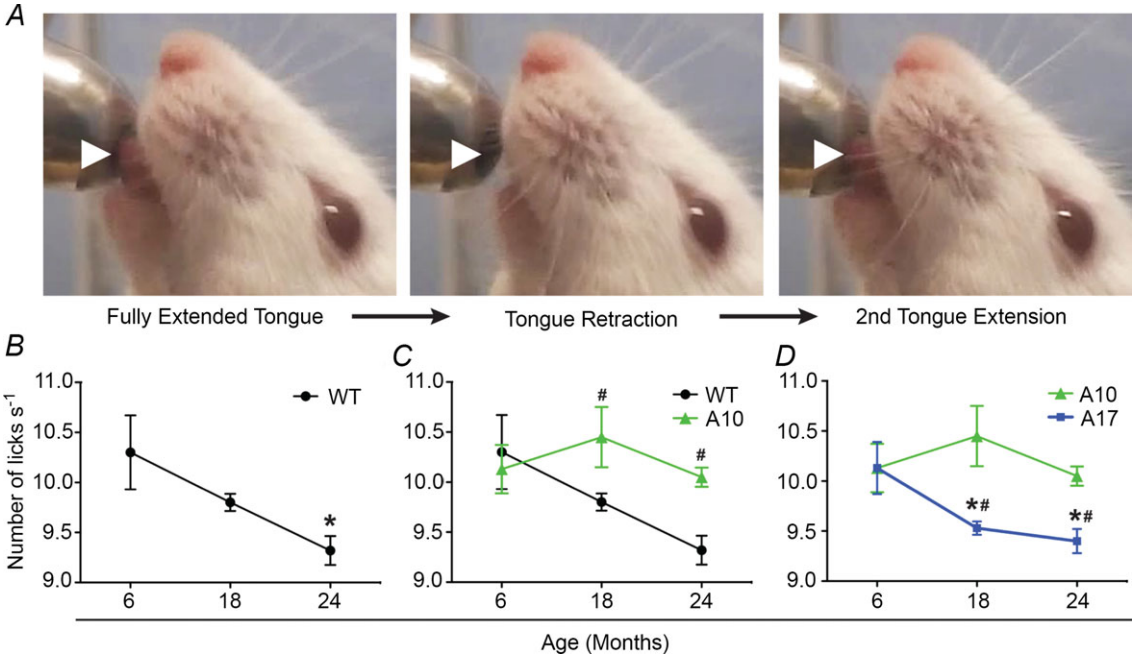

Figure 6. Overexpression of WT A10 PABPN1 protects against age- and muscular dystrophy-related dysphagia
A, single lick episode is depicted using still frames from a representative lick assay video. White arrowheads highlight the extension and retraction of the tongue. *B–D*, quantification of lick rates of WT, A10-WT or A17-MUT mice at 6, 18 and 24 months of age. Data are means ± SEM from 3 to 13 mice. *B*, WT lick rates significantly decreased at 24 months of age ($^{*}P < 0.05$). *C*, overexpression of WT A10 PABPN1 provided a protective effect on lick rates at both 18 and 24 months of age ($^{\#}P < 0.05$) when compared to WT mice at these time points. Data from WT and A10-WT mice. *D*, lick rates of A17-MUT mice significantly decreased at 18 and 24 months of age ($^{*}P < 0.05$) and were significantly impaired at these time points compared to A10-WT mice ($^{\#}P < 0.05$). A10-WT, wild-type A10.1 PABPN1 overexpression transgenic mouse; A17-MUT, mutant A17.1 PABPN1 overexpression transgenic mouse; PABN1, polyadenylate binding nuclear protein 1; WT, wild-type.

OPMD in humans (Anvar *et al.* 2013; Raz *et al.* 2014), suggesting a connection between disease and diminished PABPN1 levels in certain muscles. Our studies suggest that alleviating age- or OPMD-related PABPN1 loss with overexpression of wild-type A10 PABPN1 could potentially prevent muscle loss in the human laryngopharynx and ameliorate one of the most devastating symptoms of OPMD.

Myofibre size in the muscles of the laryngopharynx in the A10-WT was associated with an increased number of centrally located nuclei in myofibres. Neither the enhanced size phenotype nor the corresponding increase in the number of central myonuclei was observed in any other pharyngeal region of A10-WT mice. Two mechanisms could account for the presence of the centrally located myonuclei, either (1) ongoing basal myogenesis, or (2) regeneration due to focal myofibre injury. Other craniofacial muscles, such as the extraocular muscles, undergo continuous myofibre remodelling and contain a population of proliferative myogenic precursor cells (McLoon & Wirtschafter, 2002 , 2003; McLoon *et al.* 2004; Wirtschafter *et al.* 2004). If pharyngeal muscles have a similar myogenic precursor population and undergo myofibre remodelling, wild-type A10 overexpression in the laryngopharynx may selectively enhance the myogenic potential of these cells, thereby increasing the incidence of central myonuclei present in the A10-WT laryngopharynx. Alternately, the continuous tonic demand of the inferior pharyngeal constrictor may result in focal myofibre damage not detected in sections leading to local muscle regeneration and an increase of centrally located myonuclei. Further studies are needed to distinguish between these two possibilities.

Pharyngeal location results in variable sensitivity to mutant A17 polyadenylate binding nuclear protein 1 overexpression

Using the A17-MUT OPMD mouse model (Davies *et al.* 2008), we analysed the effects of mutant A17 PABPN1 overexpression on pharyngeal muscle growth. Mutant A17 PABPN1 overexpression adversely affected myofibre size in both the oro- and laryngopharynx at both 2 and 12 months of age relative to overexpression of wild-type A10 PABPN1. However, by 24 months of age, A10-WT oro- and laryngopharyngeal myofibres underwent atrophy and demonstrated a similar myofibre distribution as the A17-MUT animals, suggesting that age-related changes eventually nullified the positive growth effect of wild-type A10 PABPN1 overexpression in the oropharynx. Meanwhile, minimal to no effect of mutant A17 PABPN1 on myofibre size was observed in the palatopharyngeus of the nasopharynx regardless of age. Despite the fact that the palatopharyngeal muscle spans both the nasal and oral pharynxes, impairment of muscle growth was only observed in the oropharyngeal region of the palatopharyngeal muscle in 12-month-old A17-MUT mice. Regional differences in the effect of mutant A17 PABPN1 on myofibre size within the palatopharyngeal muscle are probably related to the unique functional demands of the oral *versus* the nasal pharynx. In the nasal pharynx, the palatopharyngeus merges with the stylopharyngeus and salpingopharyngeus to elevate the soft palate cranially and caudally as one collective unit. However, in the oral pharynx, the palatopharyngeal muscle splits into two separate heads that are no longer associated with the soft palate. This anatomical division of the palatopharyngeus within the oropharynx could exert unique physiological demands on these muscles and contribute to the region-dependent sensitivity of the palatopharyngeus to mutant A17 PABPN1 overexpression. Interestingly, overexpression of mutant A17 PABPN1 affected the muscles of the laryngopharynx in a different manner. While overexpression of wild-type A10 PABPN1 increased myofibre size at all observed ages, no increase was observed upon overexpression of mutant A17 PABPN1, which could indicate that the alanine expansion in mutant A17 PABPN1 disrupts its ability to enhance growth. Muscles of the laryngopharynx are adversely affected in patients with OPMD (Blakeley *et al.* 1968; Montgomery & Lynch, 1971; Dayal & Freeman, 1976; Little & Perl, 1982; Périé *et al.* 2006), yet it is unknown whether oropharyngeal muscle growth is adversely affected with mutant PABPN1 expression in humans. Studies assessing oropharyngeal muscle growth in patients with OPMD are needed to assess whether oropharyngeal muscles would also be viable therapeutic targets for treating OPMD-related dysphagia.

Overexpression of wild-type A10 polyadenylate binding nuclear protein 1 prevents the development of age-related dysphagia

Because no direct assays for measuring pharyngeal swallow function were available, we utilized an established oral dysphagia model that analyses lick rates (Lever *et al.* 2009, 2010) to assess indirectly the effects of ageing and muscular dystrophy on pharyngeal function. We observed that both the wild-type and A17-MUT mice developed dysphagia with age; however, muscle-specific overexpression of wild-type A10 PABPN1 protected against age-associated impairments in swallowing. Given that wild-type A10 PABPN1 overexpression protects against both age- and OPMD-dependent decreases in swallow function, as well as myofibre size, the development of therapies directed at modulating region-specific PABPN1 expression in dysphagic patients might be indicated.

Summary

We demonstrate that murine pharyngeal muscles exhibit unique phenotypes in response to ageing and muscular dystrophy related to their location within the pharynx. The pronounced protective effects from muscle-specific wild-type A10 PABPN1 overexpression on pharyngeal muscle growth and swallow function emphasize the integral role of pharyngeal muscles in swallow physiology. Additionally, our studies suggest mice are an excellent model organism in which to study molecular mechanisms underlying the changes in pharyngeal muscle physiology that occur with ageing and disease. Given the availability of numerous mutant and transgenic mice, future studies addressing the molecular and cellular biology of pharyngeal muscle could lead to new therapeutic options for individuals with dysphagia.

References

Aherne W, Ayyar DR, Clarke PA & Walton JN (1971). Muscle fiber size in normal infants, children and adolescents. An autopsy study. *J Neurol Sci* **14**, 171–182.

Aloysius A, Born P, Kinali M, Davis T, Pane M & Mercuri E (2008). Swallowing difficulties in Duchenne muscular dystrophy: indications for feeding assessment and outcome of videofluroscopic swallow studies. *Eur J Paediatr Neurol* **12**, 239–245.

Anvar SY, Raz Y, Verway N, van der Sluijs B, Venema A, Goeman JJ, Vissing J, van der Maarel SM, t Hoen PAC, van Engelen BGM & Raz V (2013). A decline in PABPN1 induces progressive muscle weakness in oculopharyngeal muscle dystrophy and in muscle aging. *Aging (Albany NY)* **5**, 412–426.

Apponi LH, Corbett AH & Pavlath GK (2013). Control of mRNA stability contributes to low levels of nuclear poly(A) binding protein 1 (PABPN1) in skeletal muscle. *Skelet Muscle* **3**, 23.

Apponi LH, Leung SW, Williams KR, Valentini SR, Corbett AH & Pavlath GK (2010). Loss of nuclear poly(A)-binding protein 1 causes defects in myogenesis and mRNA biogenesis. *Hum Mol Genet* **19**, 1058–1065.

Bachmann G, Streppel M, Krug B & Neuen-Jacob E (2001). Cricopharyngeal muscle hypertrophy associated with florid myositis. *Dysphagia* **16**, 244–248.

Banerjee A, Apponi LH, Pavlath GK & Corbett AH (2013). PABPN1: molecular function and muscle disease. *FEBS J* **280**, 4230–4250.

Blakeley WR, Garety EJ & Smith DE (1968). Section of the cricopharyngeus muscle for dysphagia. *Arch Surg* **96**, 745–762.

Bloem BR, Lagaay AM, van Beek W, Haan J, Roos RA & Wintzen AR (1990). Prevalence of subjective dysphagia in community residents aged over 87. *BMJ* **300**, 721–722.

Brais B, Bouchard JP, Xie YG, Rochefort DL, Chrétien N, Tomé FM, Lafrenière RG, Rommens JM, Uyama E, Nohira O, Blumen S, Korczyn AD, Heutink P, Mathieu J, Duranceau A, Codère F, Fardeau M, Rouleau GA & Korcyn AD (1998). Short GCG expansions in the PABP2 gene cause oculopharyngeal muscular dystrophy. *Nat Genet* **18**, 164–167.

Bredman JJ, Weijs WA, Korfage HA, Brugman P & Moorman AF (1992). Myosin heavy chain expression in rabbit masseter muscle during postnatal development. *J Anat* **180** (Pt 2), 263–274.

Butler-Browne GS, Eriksson PO, Laurent C & Thornell LE (1988). Adult human masseter muscle fibers express myosin isozymes characteristic of development. *Muscle Nerve* **11**, 610–620.

Davies JE, Wang L, Garcia-Oroz L, Cook LJ, Vacher C, O'Donovan DG & Rubinsztein DC (2005). Doxycycline attenuates and delays toxicity of the oculopharyngeal muscular dystrophy mutation in transgenic mice. *Nat Med* **11**, 672–677.

Davies JE, Sarkar S & Rubinsztein DC (2008). Wild-type PABPN1 is anti-apoptotic and reduces toxicity of the oculopharyngeal muscular dystrophy mutation. *Hum Mol Genet* **17**, 1097–1108.

Davis MV, Merati AL, Jaradeh SS & Blumin JH (2007). Myosin heavy chain composition and fiber size of the cricopharyngeus muscle in patients with achalasia and normal subjects. *Ann Otol Rhinol Laryngol* **116**, 643–646.

Dayal VS & Freeman J (1976). Cricopharyngeal myotomy for dysphagia in oculopharyngeal muscular dystrophy. Report of a case. *Arch Otolaryngol* **102**, 115–116.

Donner MW, Bosma JF & Robertson DL (1985). Anatomy and physiology of the pharynx. *Gastrointest Radiol* **10**, 196–212.

Dutta CR & Basmajian JV (1960). Gross and histological structure of the pharyngeal constrictors in the rabbit. *Anat Rec* **137**, 127–134.

Eicher PS, McDonald-Mcginn DM, Fox CA, Driscoll DA, Emanuel BS & Zackai EH (2000). Dysphagia in children with a 22q11.2 deletion: unusual pattern found on modified barium swallow. *J Pediatr* **137**, 158–164.

Ekberg O, Ekman M, Eriksson LI, Malm R, Sundman E & Arner A (2009). An in vitro model for studying neuromuscular transmission in the mouse pharynx. *Dysphagia* **24**, 32–39.

Ertekin C & Aydogdu I (2003). Neurophysiology of swallowing. *Clin Neurophysiol* **114**, 2226–2244.

Ertekin C, Yuceyar N & Aydogdu I (1998). Clinical and electrophysiological evaluation of dysphagia in myasthenia gravis. *J Neurol Neurosurg Psychiatry* **65**, 848–856.

Eslick GD & Talley NJ (2008). Dysphagia: epidemiology, risk factors and impact on quality of life – a population-based study. *Aliment Pharmacol Ther* **27**, 971–979.

Gidaro T, Negroni E, Périé S, Mirabella M, Lainé J, Lacau St Guily J, Butler-Browne G, Mouly V & Trollet C (2013). Atrophy, fibrosis, and increased PAX7-positive cells in pharyngeal muscles of oculopharyngeal muscular dystrophy patients. *J Neuropathol Exp Neurol* **72**, 234–243.

Himmelreich HA (1973). [The palatopharyngeal muscle of mammals]. *Gegenbaurs Morphol Jahrb* **119**, 172–212.

Holland G, Jayasekeran V, Pendleton N, Horan M, Jones M & Hamdy S (2011). Prevalence and symptom profiling of oropharyngeal dysphagia in a community dwelling of an elderly population: a self-reporting questionnaire survey. *Dis Esophagus* **24**, 476–480.

Hyodo M, Yumoto E, Kawakita S & Yamagata T (1999). Postnatal changes in the types of muscle fiber in the canine inferior pharyngeal constrictor. *Acta Otolaryngol* **119**, 843–846.

Johnson BD, Wilson LE, Zhan WZ, Watchko JF, Daood MJ & Sieck GC (1994). Contractile properties of the developing diaphragm correlate with myosin heavy chain phenotype. *J Appl Physiol* **77**, 481–487.

Kawashima K, Motohashi Y & Fujishima I (2004). Prevalence of dysphagia among community-dwelling elderly individuals as estimated using a questionnaire for dysphagia screening. *Dysphagia* **19**, 266–271.

Kirberger RM, Steenkamp G, Spotswood TC, Boy SC, Miller DB & van Zyl M (2006). Stenotic nasopharyngeal dysgenesis in the dachshund: seven cases (2002–2004). *J Am Anim Hosp Assoc* **119**, 290–297.

Leese G & Hopwood D (1986). Muscle fiber typing in the human pharyngeal constrictors and oesophagus: the effect of ageing. *Acta Anat (Basel)* **127**, 77–80.

Lever TE, Gorsek A, Cox KT, O'Brien KF, Capra NF, Hough MS & Murashov AK (2009). An animal model of oral dysphagia in amyotrophic lateral sclerosis. *Dysphagia* **24**, 180–195.

Lever TE, Simon E, Cox KT, Capra NF, O'Brien KF, Hough MS & Murashov AK (2010). A mouse model of pharyngeal dysphagia in amyotrophic lateral sclerosis. *Dysphagia* **25**, 112–126.

Lexell J, Taylor CC & Sjöström M (1988). What is the cause of the ageing atrophy? Total number, size and proportion of different fiber types studied in whole vastus lateralis muscle from 15- to 83-year-old men. *J Neurol Sci* **84**, 275–294.

Lindgren S & Janzon L (1991). Prevalence of swallowing complaints and clinical findings among 50-79-year-old men and women in an urban population. *Dysphagia* **6**, 187–192.

Little BW & Perl DP (1982). Oculopharyngeal muscular dystrophy. An autopsied case from the French-Canadian kindred. *J Neurol Sci* **53**, 145–158.

Logemann JA (2007). Swallowing disorders. *Best Pract Res Clin Gastroenterol* **21**, 563–573.

Martin BJ, Corlew MM, Wood H, Olson D, Golopol LA, Wingo M & Kirmani N (1994). The association of swallowing dysfunction and aspiration pneumonia. *Dysphagia* **9**, 1–6.

McLoon LK (1998). Muscle fiber type compartmentalization and expression of an immature myosin isoform in the sternocleidomastoid muscle of rabbits and primates. *J Neurol Sci* **156**, 3–11.

McLoon LK & Wirtschafter JD (2002). Continuous myonuclear addition to single extraocular myofibers in uninjured adult rabbits. *Muscle Nerve* **25**, 348–358.

McLoon LK & Wirtschafter J (2003). Activated satellite cells in extraocular muscles of normal adult monkeys and humans. *Invest Ophthalmol Vis Sci* **44**, 1927–1932.

McLoon LK, Rowe J, Wirtschafter J & McCormick KM (2004). Continuous myofiber remodeling in uninjured extraocular myofibers: myonuclear turnover and evidence for apoptosis. *Muscle Nerve* **29**, 707–715.

Miller AJ. (2008). The neurobiology of swallowing and dysphagia. *Dev Disabil Res Rev* **14**, 77–86.

Montgomery WW & Lynch JP (1971). Oculopharyngeal muscular dystrophy treated by inferior constrictor myotomy. *Trans Am Acad Ophthalmol Otolaryngol* **75**, 986–993.

Mootoosamy RC & Dietrich S (2002). Distinct regulatory cascades for head and trunk myogenesis. *Development* **129**, 573–583.

Mu L & Sanders I (2002). Muscle fiber-type distribution pattern in the human cricopharyngeus muscle. *Dysphagia* **17**, 87–96.

Mu L, Su H, Wang J & Sanders I (2007). Myosin heavy chain-based fiber types in the adult human cricopharyngeus muscle. *Muscle Nerve* **35**, 637–648.

Mu L, Sobotka S, Chen J, Su H, Sanders I, Adler CH, Shill HA, Caviness JN, Samanta JE, Beach TG & Consortium APasD (2012). Altered pharyngeal muscles in Parkinson disease. *J Neuropathol Exp Neurol* **71**, 520–530.

Nakano T & Muto H (1985). Anatomical observations in the pharynx of the mouse with special reference to the nasopharyngeal hiatus (Wood Jones). *Acta Anat (Basel)* **121**, 147–152.

Noden DM & Francis-West P (2006). The differentiation and morphogenesis of craniofacial muscles. *Dev Dyn* **235**, 1194–1218.

Nozaki S, Umaki Y, Sugishita S, Tatara K, Adachi K & Shinno S (2007). Videofluorographic assessment of swallowing function in patients with Duchenne muscular dystrophy. *Rinsho Shinkeigaku* **47**, 407–412.

Périé S, Mamchaoui K, Mouly V, Blot S, Bouazza B, Thornell L-E, St Guily JL & Butler-Browne G (2006). Premature proliferative arrest of cricopharyngeal myoblasts in oculo-pharyngeal muscular dystrophy: Therapeutic perspectives of autologous myoblast transplantation. *Neuromuscul Disord* **16**, 770–781.

Prasse JE & Kikano GE (2009). An overview of pediatric dysphagia. *Clin Pediatr* **48**, 247–251.

Raz V, Buijze H, Raz Y, Verwey N, Anvar SY, Aartsma-Rus A & van der Maarel SM (2014). A novel feed-forward loop between ARIH2 E3-ligase and PABPN1 regulates aging-associated muscle degeneration. *Am J Pathol* **184**, 1119–1131.

Reiser PJ, Moss RL, Giulian GG & Greaser ML (1985*a*). Shortening velocity and myosin heavy chains of developing rabbit muscle fibers. *J Biol Chem* **260**, 14403–14405.

Reiser PJ, Moss RL, Giulian GG & Greaser ML (1985*b*). Shortening velocity in single fibers from adult rabbit soleus muscles is correlated with myosin heavy chain composition. *J Biol Chem* **260**, 9077–9080.

Robbins J, Langmore S, Hind JA & Erlichman M (2002). Dysphagia research in the 21st century and beyond: proceedings from Dysphagia Experts Meeting, August 21, 2001. *J Rehabil Res Dev* **39**, 543–548.

Robinson DO, Hammans SR, Read SP & Sillibourne J (2005). Oculopharyngeal muscular dystrophy (OPMD): analysis of the PABPN1 gene expansion sequence in 86 patients reveals 13 different expansion types and further evidence for unequal recombination as the mutational mechanism. *Hum Genet* **116**, 267–271.

Rubesin SE, Jessurun J, Robertson D, Jones B, Bosma JF & Donner MW (1987). Lines of the pharynx. *Radiographics* **7**, 217–237.

Scapolo PA, Rowlerson A, Mascarello F & Veggetti A (1991). Neonatal myosin in bovine and pig tensor tympani muscle fibers. *J Anat* **178**, 255–263.

Schmalbruch H (1976). The morphology of regeneration of skeletal muscles in the rat. *Tissue Cell* **8**, 673–692.

Talmadge RJ & Roy RR (1993). Electrophoretic separation of rat skeletal muscle myosin heavy-chain isoforms. *J Appl Physiol* **75**, 2337–2340.

Taylor EW (1915). Progressive vagus-glossopharyngeal paralysis with ptosis: contribution to group of family diseases. *J Nerv Ment Dis* **42**, 129–139.

Trollet C, Anvar SY, Venema A, Hargreaves IP, Foster K, Vignaud A, Ferry A, Negroni E, Hourde C, Baraibar MA, 't Hoen PAC, Davies JE, Rubinsztein DC, Heales SJ, Mouly V, van der Maarel SM, Butler-Browne G, Raz V & Dickson G (2010). Molecular and phenotypic characterization of a mouse model of oculopharyngeal muscular dystrophy reveals severe muscular atrophy restricted to fast glycolytic fibers. *Hum Mol Genet* **19**, 2191–2207.

Victor M, Hayes R & Adams RD (1962). Oculopharyngeal muscular dystrophy. A familial disease of late life characterized by dysphagia and progressive ptosis of the evelids. *N Engl J Med* **267**, 1267–1272.

Wada KI, Katsuta S & Soya H (2003). Natural occurrence of myofiber cytoplasmic enlargement accompanied by decrease in myonuclear number. *Jpn J Physiol* **53**, 145–150.

Wieczorek DF, Periasamy M, Butler-Browne GS, Whalen RG & Nadal-Ginard B (1985). Co-expression of multiple myosin heavy chain genes, in addition to a tissue-specific one, in extraocular musculature. *J Cell Biol* **101**, 618–629.

Wirtschafter JD, Ferrington DA & McLoon LK (2004). Continuous remodeling of adult extraocular muscles as an explanation for selective craniofacial vulnerability in oculopharyngeal muscular dystrophy. *J Neuroophthalmol* **24**, 62–67.

Additional information

Competing interests

The authors have no competing interests.

Author contributions

M.E.R. and G.K.P. contributed to the conception and design of these studies. Q.L. in the laboratory of A.J.S. performed data collection, analysis and subsequent interpretation for the biochemical analysis of pharyngeal myosin heavy chain composition. M.E.R., J.H. and K.E.V. in the laboratory of G.K.P. performed all other data collections, analyses and interpretations. All authors contributed to the writing and critical revision of the manuscript.

Funding

This work was supported by National Institute of Health grants AR061987 (GP), DC005017 (AS), and DC012225 (MR).

Acknowledgements

We thank Drs A. Banerjee, A. Corbett, A. English, M. Johns III, T. Lever and R. Price for training and/or helpful discussions; E. Andreas for providing the schematic of pharyngeal anatomy; and E. Andreas, T. Swink, N. Pescatore, P. Pham and P. Devadas for technical assistance. In addition, we thank Dr D. Rubensztein for the generous gift of the A10.1 and A17.1 PABPN1 mice.

Supporting information

Supporting Video 1. Representative lick assay video utilized for lick rate quantification. Video was edited using iMovie 9.0.4 and saved as a MPEG-4 file.